Resumed predictions for differential rates of inclusive B-meson decays

Continuation of arXiv:2211.07663

Bahman Dehnadi (DESY), **Ivan Novikov** (KIT), Frank J. Tackmann (DESY)

Loops and Legs in Quantum Field Theory

2024-04-18

Improved theoretical description of inclusive $B \to X_s\gamma$ and $B \to X_u l\bar{\nu}$ decays enables a more reliable future determination of $|V_{ub}|$

- Extraction of $|V_{ub}|$ CKM matrix element from B-meson decay $B \to X_u l\bar{\nu}$
- Factorization of decay rates in Soft-Collinear Effective Theory (SCET) into perturbative and nonperturbative ingredients.
- Impact of different definitions of the b-quark mass m_b
- Improved theoretical results for *differential* $B \to X_s\gamma$ and $B \to X_u l\bar{\nu}$ decay rates

Cabibbo-Kobayashi-Maskawa matrix

$$\begin{pmatrix} |V_{ud}| & |V_{us}| & |V_{ub}| \\ |V_{cd}| & |V_{cs}| & |V_{cb}| \\ |V_{td}| & |V_{ts}| & |V_{tb}| \end{pmatrix} = \begin{pmatrix} 973.73 \pm 0.31 & 224.3 \pm 0.8 & 3.82 \pm 0.2 \\ 221 \pm 4 & 975 \pm 6 & 40.8 \pm 1.4 \\ 8.6 \pm 0.2 & 41.5 \pm 9 & 1014 \pm 29 \end{pmatrix} \cdot 10^{-3}$$

$|V_{ub}|$ is the smallest element of the CKM matrix,
and is known with the largest relative uncertainty.

CKM unitarity triangle

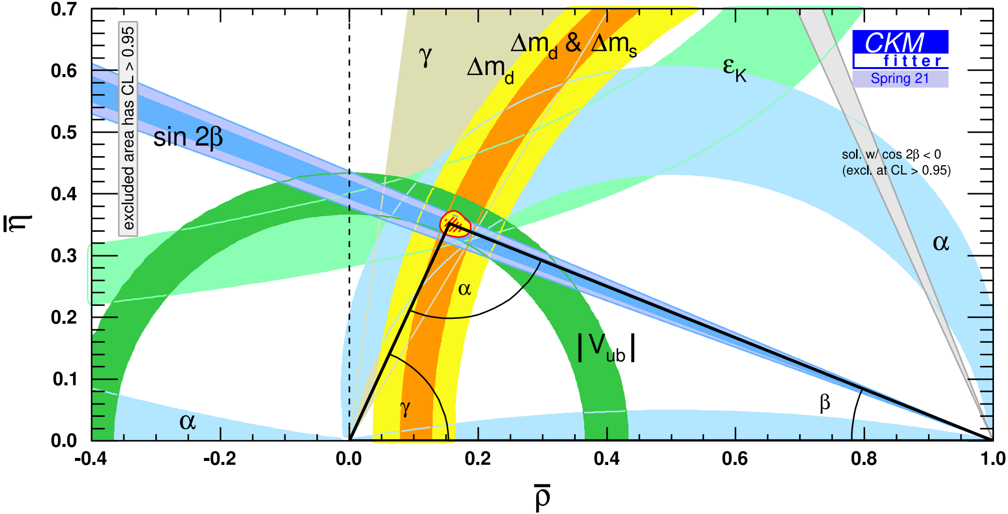

A more precise determination of $|V_{ub}|$ is important to constrain the small side of the CKM unitarity triangle.

$B \to X_s\gamma$

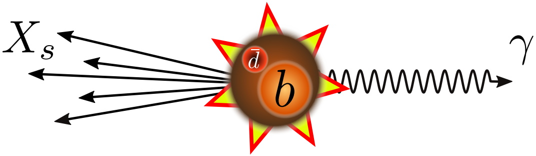

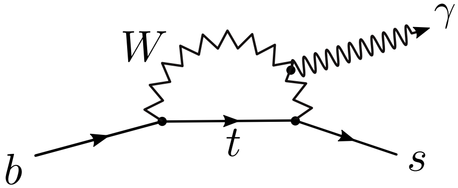

$B \to X_u l\bar{\nu}$ $(l \in \{e, \mu\})$

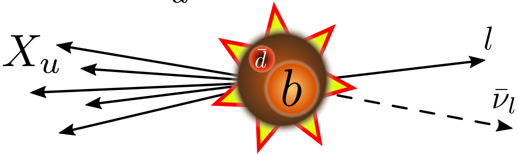

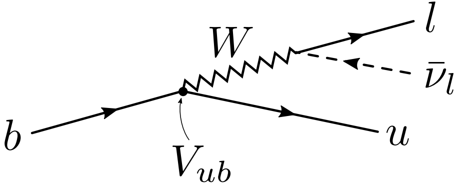

Properties of the b-quark can be determined in B-meson decays, such as $B \to X_s\gamma$ and $B \to X_u l\bar{\nu}$.

this work

$$B \to X_u l\bar{\nu}$$

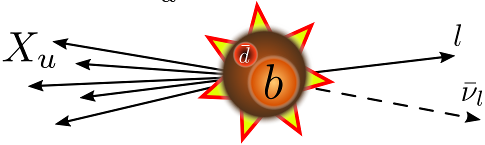

inclusive $$\boxed{\sum_{X_u} \mathrm{d}\Gamma(B \to X_u l\bar{\nu})}$$

exclusive
$$\mathrm{d}\Gamma(B \to \pi l\bar{\nu})$$
$$\mathrm{d}\Gamma(B \to \rho l\bar{\nu})$$
$$\mathrm{d}\Gamma(B_s \to K l\bar{\nu})$$

Determinations of $|V_{ub}|$ from $B \to X_u l\bar{\nu}$ can be classified as inclusive or exclusive.
Matteo Fael, Jian Wang, and Long Chen presented total Γ and $\mathrm{d}\Gamma/\mathrm{d}q^2$ at $\mathrm{N^3LO}$.
Our work is focused on the inclusive decay rate, but *differential* in kinematics of $l, \bar{\nu}, \gamma$.

Tension between inclusive and exclusive determinations of $|V_{ub}|$

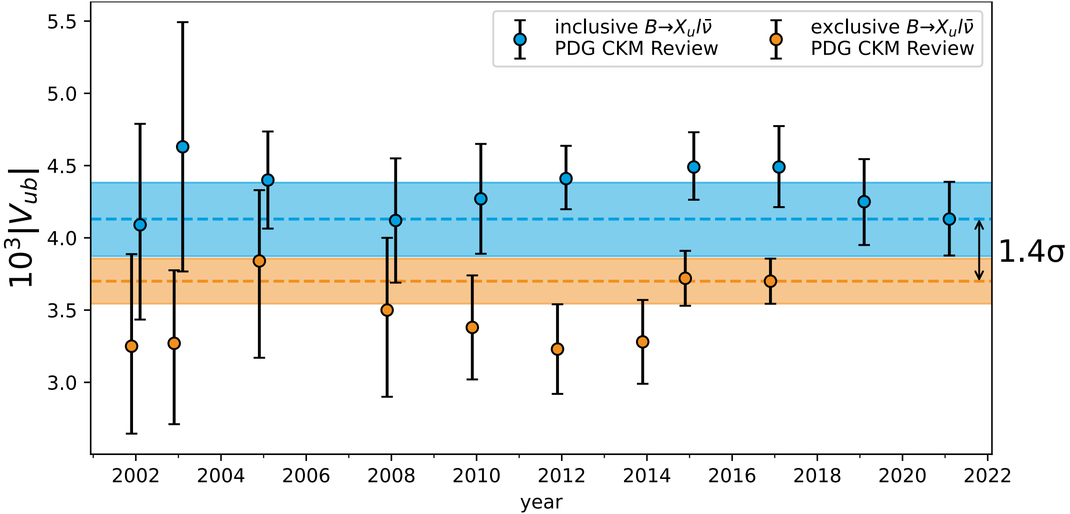

In spite of increasing precision there's a persistent tension between inclusive and exclusive determinations of $|V_{ub}|$

$B \to X_c l\bar{\nu}$ background

[Phys.Rev.D 104 (2021), 1, 012008, Belle collaboration]

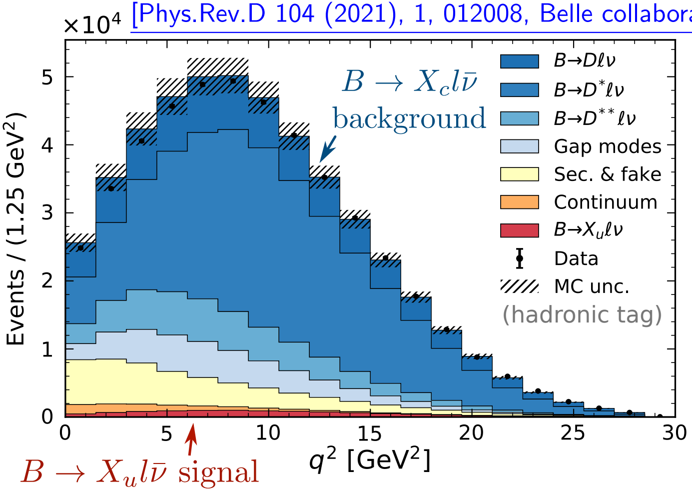

The signal of $B \to X_u l\bar{\nu}$ is obscured by large $B \to X_c l\bar{\nu}$ background, which is relatively enhanced by a factor $|V_{cb}/V_{ub}|^2 \sim 100$.

Reducing $B \to X_c l \bar{\nu}$ background

[Phys.Rev.D 104 (2021), 1, 012008, Belle collaboration]

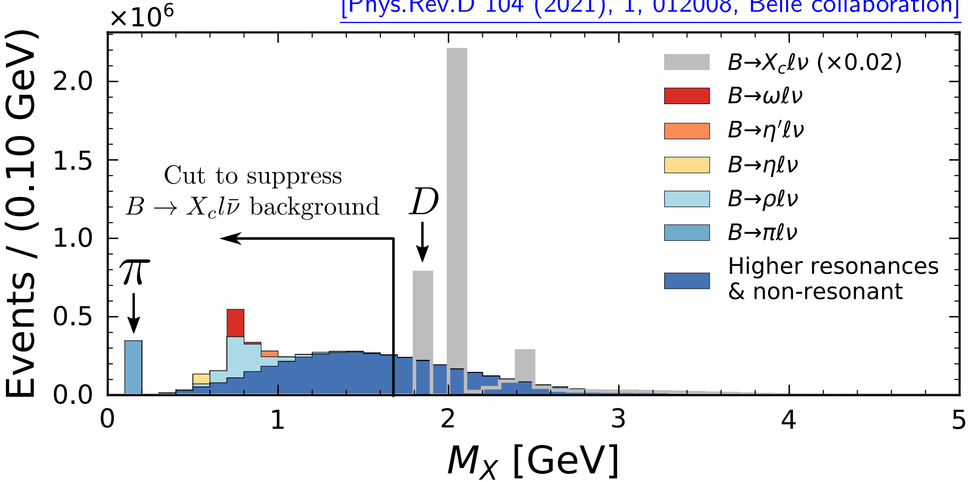

Because the lightest u-meson, π, is lighter than the lightest c-meson, D, the $B \to X_c l \bar{\nu}$ background is absent in the endpoint region of $B \to X_u l \bar{\nu}$.

$$B \to X_u l \bar{\nu}$$

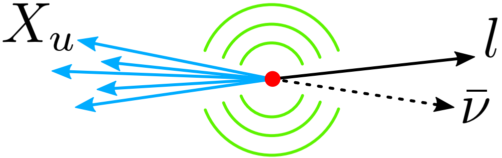

$$B \to X_s \gamma$$

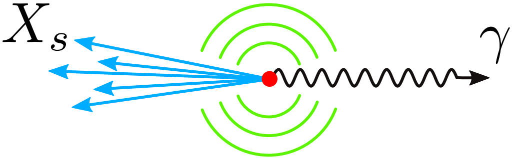

In the endpoint region the final hadronic state X consists of a strongly boosted jet and wide-angle soft radiation.

Factorization in the endpoint region

$$B \to X_u l \bar{\nu}$$

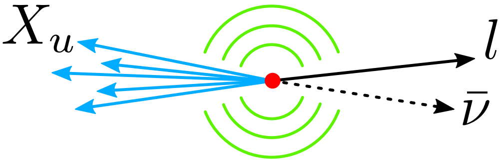

$$B \to X_s \gamma$$

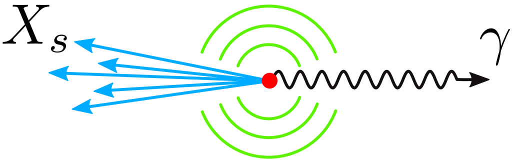

$\mu_H \sim m_b$ $\quad$ $\mu_J \sim m_X \sim \sqrt{m_b \Lambda_{\mathrm{QCD}}}$ $\quad$ $\mu_S \sim \Lambda_{\mathrm{QCD}}$

Soft-Collinear Effective Theory (SCET) separates physics at hard, jet, and soft energy scales.

$$B \to X_u l \bar{\nu}$$

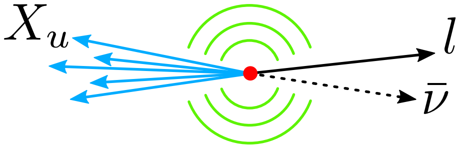

$$B \to X_s \gamma$$

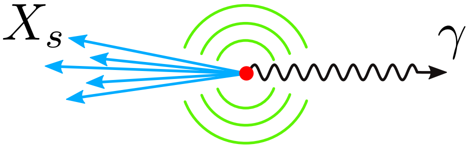

$$\mu_H \sim m_b \qquad \mu_J \sim m_X \sim \sqrt{m_b \Lambda_{\mathrm{QCD}}} \qquad \mu_S \sim \Lambda_{\mathrm{QCD}}$$

$$\mathrm{d}\Gamma \propto \underbrace{\overbrace{H}^{\text{process-specific}} \times \mathrlap{\overbrace{}^{\text{universal}}} J \otimes S}_{\text{perturbative}} \otimes \underbrace{F}_{\text{nonperturbative}}$$

As a result, the transition probabilities factorize into perturbative hard, jet, (partonic) soft functions, and nonperturbative shape function.

Shape function from $B \to X_s\gamma$ photon energy spectrum

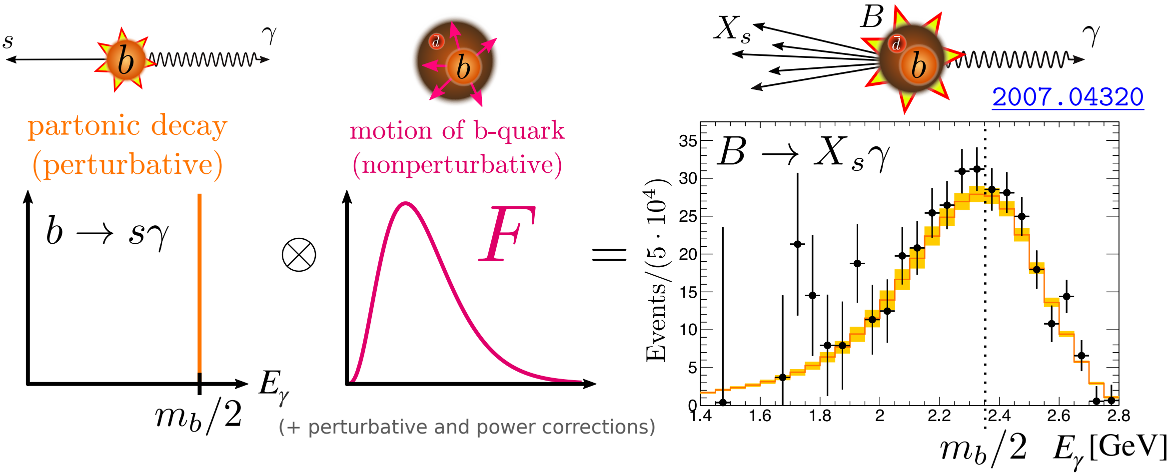

The nonperturbative shape function F can be extracted from measurements of $B \to X_s\gamma$ photon energy spectrum.

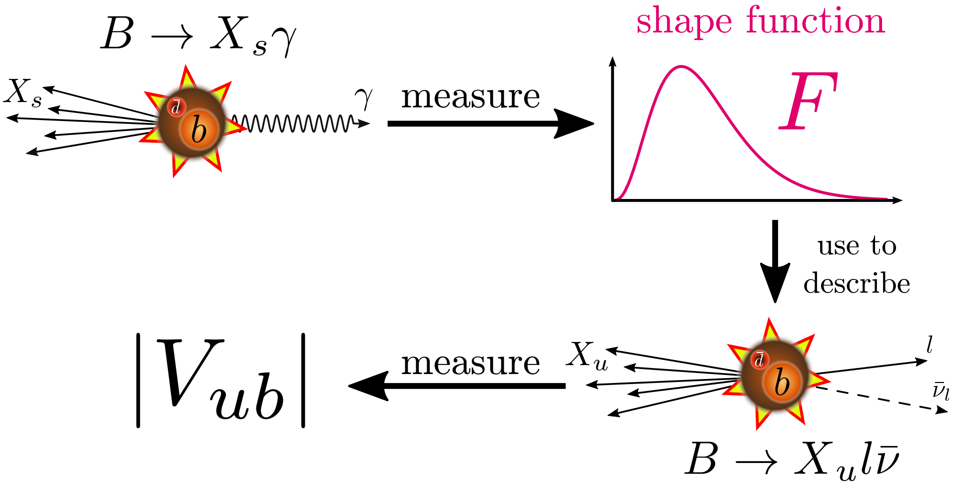

The shape function F can be extracted from $B \to X_s\gamma$ spectrum and used to describe $B \to X_u l\bar{\nu}$, which is sensitive to $|V_{ub}|$.

$$\mathrm{d}\Gamma \propto \underbrace{\Big(\overbrace{H \times J \otimes S}^{\text{SCET, resummed}} + \overbrace{W_{\text{nonsingular}}}^{\text{fixed-order}}\Big)}_{\text{reproduces full QCD when resummation is off}} \otimes F$$

SCET factorization enables resummation of singular contributions, which improves the predictions in the endpoint region. The remaining, non-singular contributions, are included at fixed order (not resummed).

ingredient	known at
$B \to X_s\gamma$	
H	2-loop
$W_{\mathrm{nonsingular}}$	2-loop
$B \to X_u l\bar{\nu}$	
H	2-loop
$W_{\mathrm{nonsingular}}$	1-loop*
universal	
J	3-loop
S	3-loop
γ_H	3-loop
γ_J	3-loop
γ_S	3-loop

3-loop corrections are parametrized with nuisance parameters c_k

$$\gamma_H = -\gamma_J - \gamma_S$$

(references in backup)

We implemented the $B \to X_s\gamma$ predictions at $\mathrm{N^3LL'}+\mathrm{N^3LO}(c_k)$ and the $B \to X_u l\bar{\nu}$ predictions at $\mathrm{N^3LL}+\mathrm{NLO}$ in the SCETLIB C++ library.

Impact of b-quark mass definition on the $B \to X_s\gamma$ photon energy spectrum

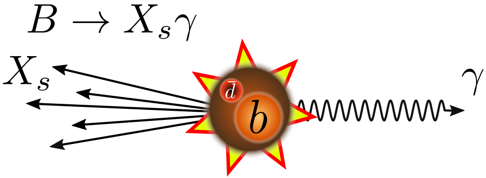

$$E_\gamma \sim \frac{m_b}{2}$$

Pole mass scheme

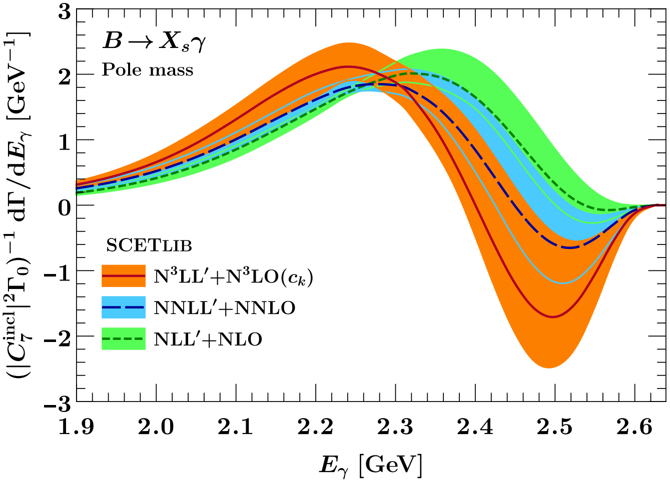

Pole mass scheme suffers from a renormalon ambiguity, and predictions in this scheme are not stable.

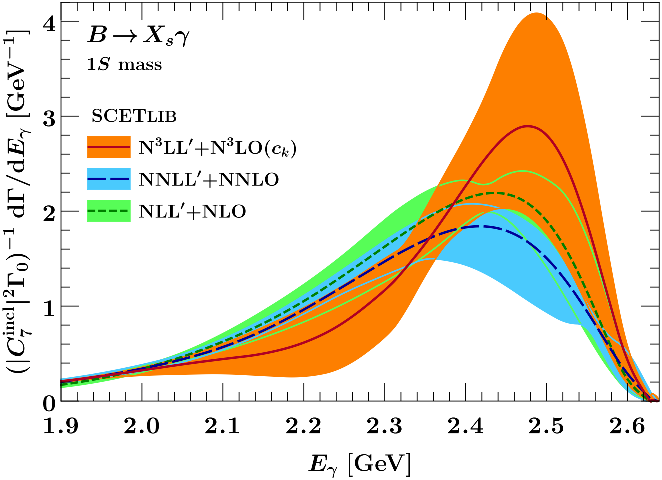

However, the $1\mathrm{S}$ mass scheme, which has been used in the $\mathrm{NNLL'+NNLO}$ shape function fit in [Bernlochner et al.: 2007.04320], starts to break down at $\mathrm{N^3LO}$

MSR mass scheme

$$m_b^{\text{pole}} - m_b^{\text{MSR}} =: \delta m_b^{\text{MSR}}(R) = R \sum_{k=1} \left(\frac{\alpha_s(R)}{\pi} \right)^k a_k^{\text{MSR}}$$

R-scale is a parameter

[A.H.Hoang, A.Jain, C.Lepenik, V.Mateu, M.Preisser, I.Scimemi, I.W.Stewart: 1704.01580]

[A.H.Hoang, A.Jain, I.Scimemi, I.W.Stewart: 0803.4214]

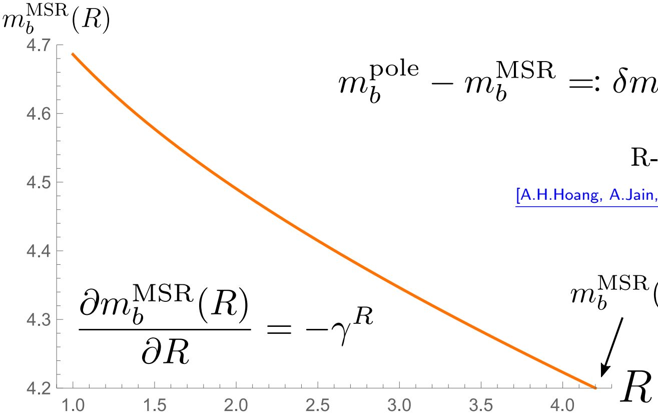

$$\frac{\partial m_b^{\text{MSR}}(R)}{\partial R} = -\gamma^R$$

$$m_b^{\text{MSR}}(\bar{m}_b) = \bar{m}_b(\bar{m}_b)$$

The MSR mass is a natural extension of the $\overline{\text{MS}}$ mass for scales below the mass of the quark.
The MSR mass $m_b^{\text{MSR}}(R)$ depends on scale R as a parameter.
Masses at different R-scales are related by the R-evolution equation.

MSR mass scheme

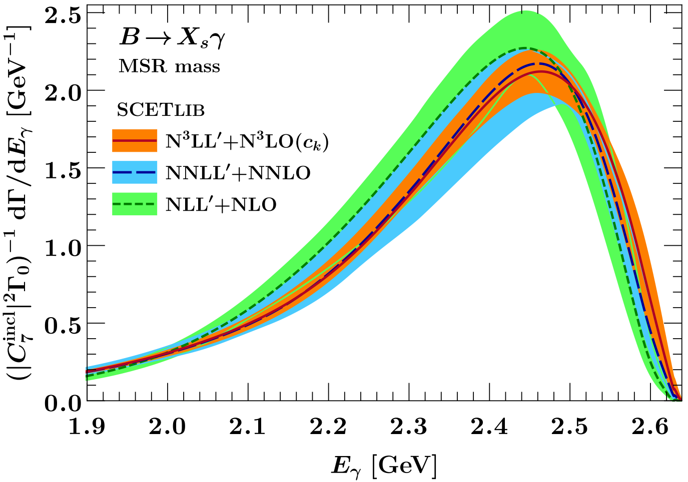

The MSR scheme yields much more stable results because we can pick the R-scale $R \sim \mu_S$

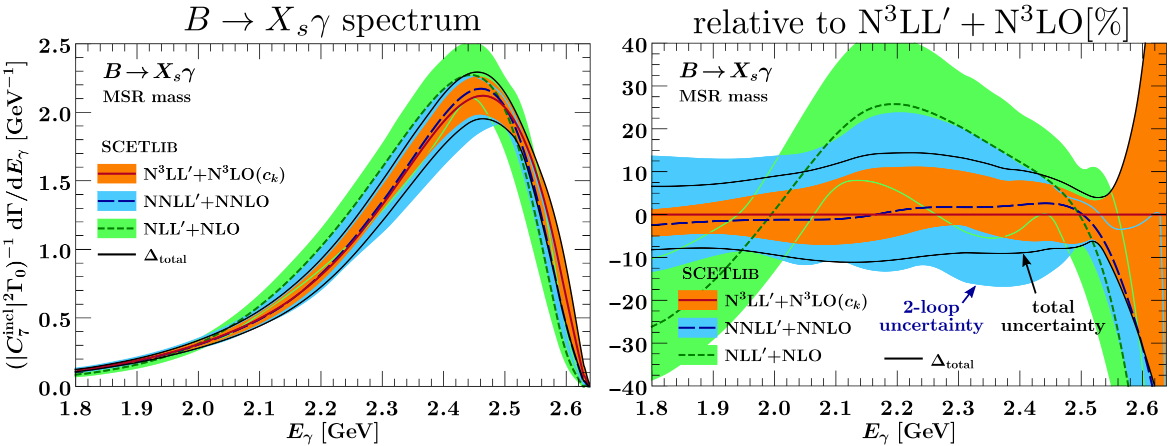

The predictions at different orders are converging well,
and the uncertainty at the highest order is reduced despite the missing 3-loop corrections

Improved predictions for inclusive $B \to X_u l \bar{\nu}$

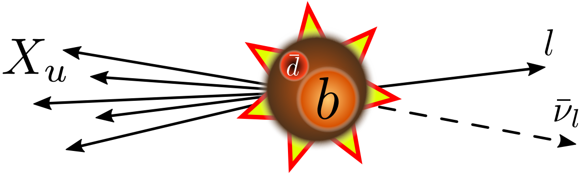

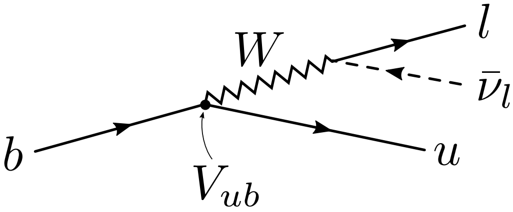

Kinematic regimes of $B \to X_u l \bar{\nu}$

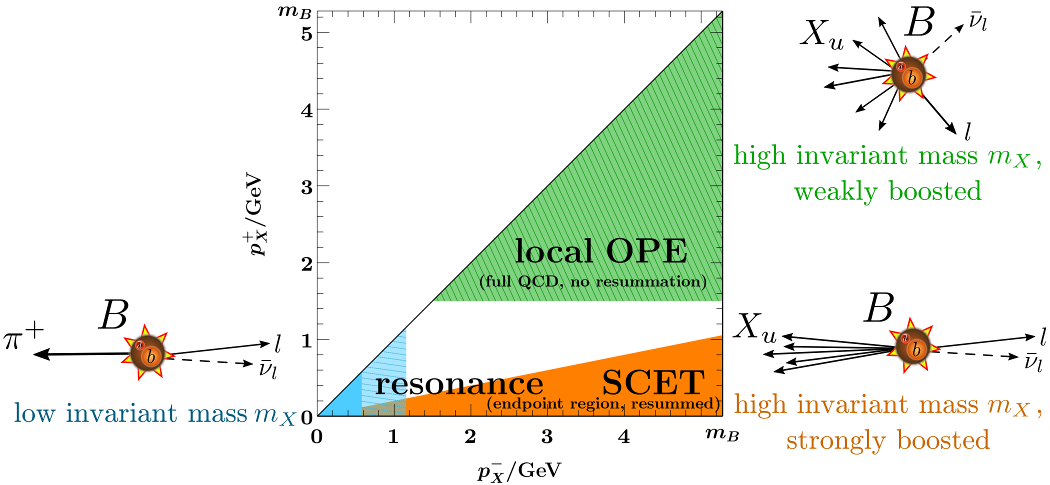

Either SCET or full QCD with local operator-product expansion (OPE) are appropriate in different kinematic regions. In the resonance region the inclusive approach is not valid.

Double-differential $B \to X_u l \bar{\nu}$ decay rate

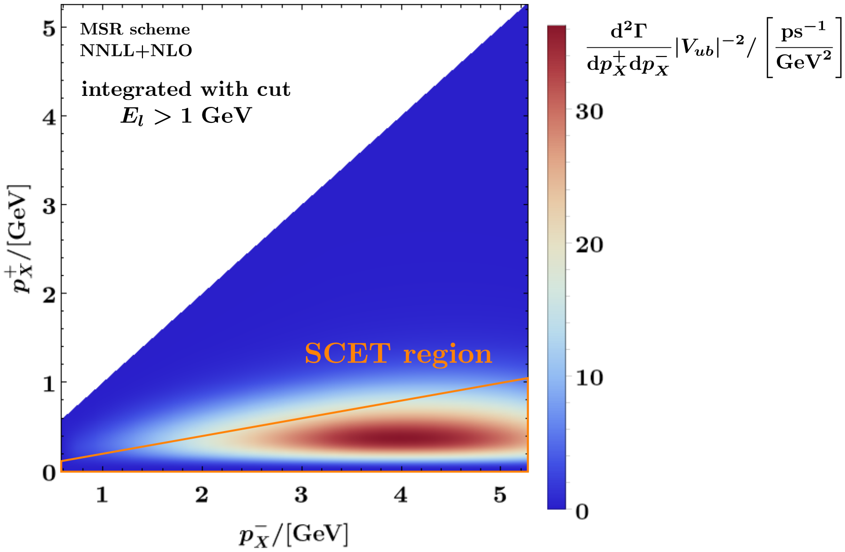

Most of the $B \to X_u l \bar{\nu}$ events are in the SCET region.

$B \to X_u l\bar{\nu}$ p_X^+ spectrum

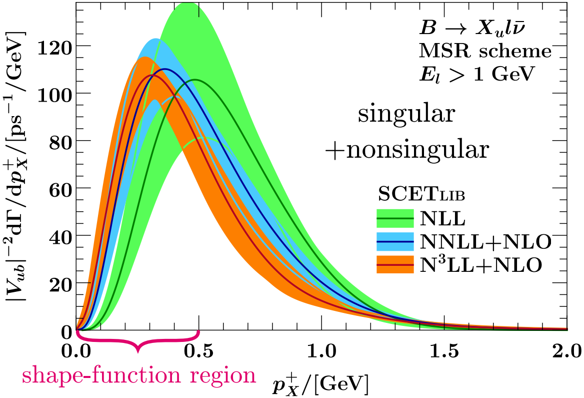

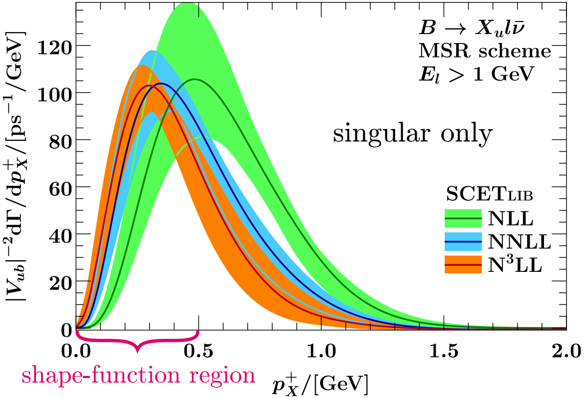

The 2-loop singular corrections reduce the theoretical uncertainty in the shape-function region.

$B \to X_u l \bar{\nu}$ lepton energy spectrum

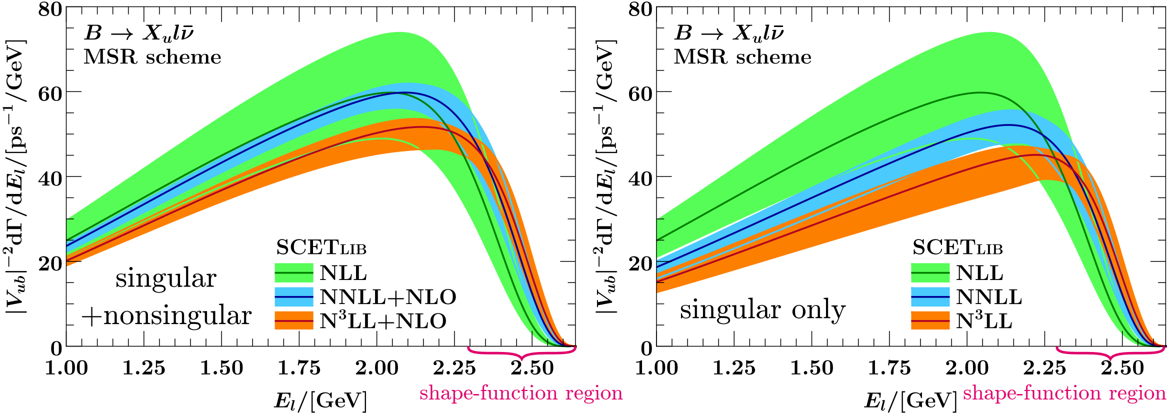

However, outside of the shape-function region, singular results by themselves are not reliable.
At the 2-loop order nonsingular corrections are also needed.

Data from [Phys.Rev.Lett. 127 (2021) 26, 261801, Belle collaboration]

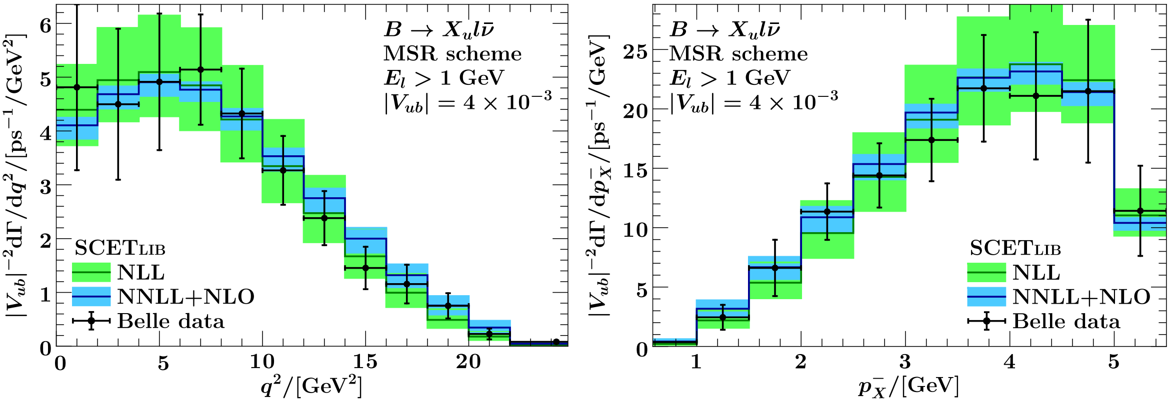

(N^{3}LL+NLO results are unreliable due to missing nonsingular contributions)

The $\mathrm{d}\Gamma/\mathrm{d}q^2$ and $\mathrm{d}\Gamma/\mathrm{d}p_X^-$ spectra, which are insensitive to the shape function F, agree with Belle measurements.

Data and right plot from [Phys.Rev.Lett. 127 (2021) 26, 261801, Belle collaboration]

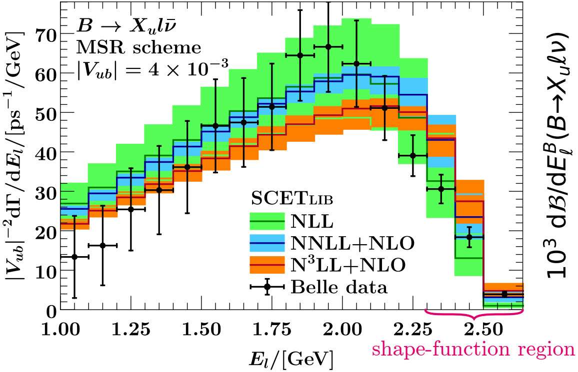

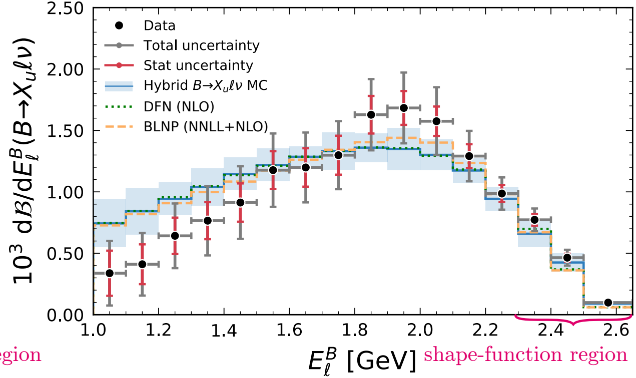

Discrepancies between theory and data are similar for different inclusive models.
The difference near the endpoint could be due to subleading shape functions.

$B \to X_u l\bar{\nu}$ p_X^+ spectrum

Data and right plot from [Phys.Rev.Lett. 127 (2021) 26, 261801, Belle collaboration]

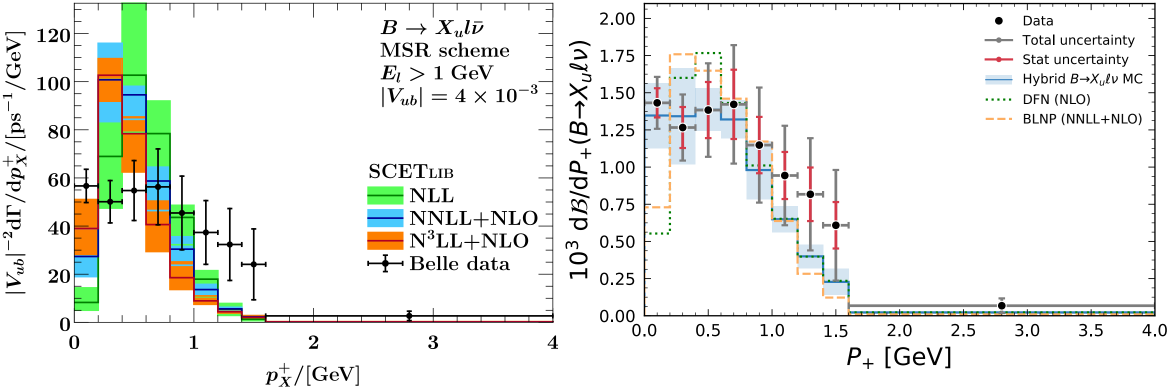

Discrepancies between theory and data are similar for all inclusive models, while the hybrid model agrees with the data. This shows that the resonant contributions are important.

$B \to X_u l\bar{\nu}$ m_X spectrum

Data and right plot from [Phys.Rev.Lett. 127 (2021) 26, 261801, Belle collaboration]

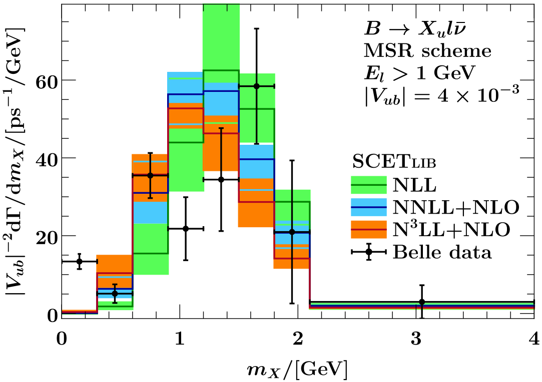

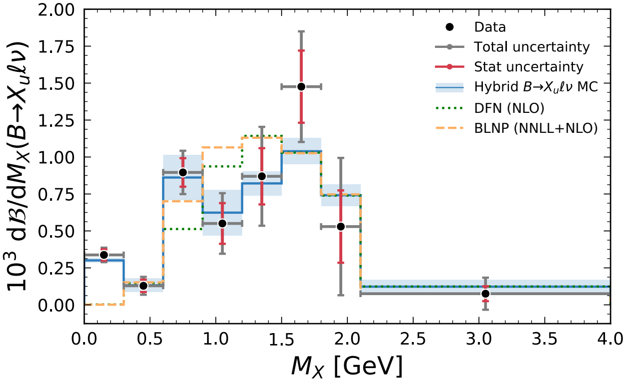

The invariant-mass spectrum $\mathrm{d}\Gamma/\mathrm{d}m_X$ is dominated by resonances and cannot be adequately described by an inclusive model.

Conclusions

- The shape function F can be determined from measurements of $B \to X_s\gamma$ decay and used to describe $B \to X_u l\bar{\nu}$ decay, which is sensitive to $|V_{ub}|$.
- The MSR mass scheme works better than the $\mathrm{1S}$ and pole schemes, especially at 3-loop order.
- Uncertainties in theoretical predictions for $B \to X_s\gamma$ decay are reduced at the 3-loop order despite some missing 3-loop corrections.
- 2-loop singular corrections reduce uncertainty of $B \to X_u l\bar{\nu}$ predictions in the SCET region
- Outside of the SCET region the 2-loop nonsingular corrections for $B \to X_u l\bar{\nu}$ are needed.
- The $B \to X_u l\bar{\nu}$ predictions are in good agreement with Belle measurements in absence of resonances.

Improved theoretical description of inclusive $B \to X_s\gamma$ and $B \to X_u l\bar{\nu}$ decays enables a more reliable future determination of $|V_{ub}|$

- The shape function F can be determined from measurements of $B \to X_s\gamma$ decay and used to describe $B \to X_u l\bar{\nu}$ decay, which is sensitive to $|V_{ub}|$.
- The MSR mass scheme works better than the $\mathrm{1S}$ and pole schemes, especially at 3-loop order.
- Uncertainties in theoretical predictions for $B \to X_s\gamma$ decay are reduced at the 3-loop order despite some missing 3-loop corrections.
- 2-loop singular corrections reduce uncertainty of $B \to X_u l\bar{\nu}$ predictions in the SCET region
- Outside of the SCET region the 2-loop nonsingular corrections for $B \to X_u l\bar{\nu}$ are needed.
- The $B \to X_u l\bar{\nu}$ predictions are in good agreement with Belle measurements in absence of resonances.

Improved theoretical description of inclusive $B \to X_s\gamma$ and $B \to X_u l\bar{\nu}$ decays enables a more reliable future determination of $|V_{ub}|$

Thank you for your attention!

Backup slides

Backup

Definition of the unitarity triangle

$$\begin{pmatrix} V_{ud} & V_{us} & V_{ub} \\ V_{cd} & V_{cs} & V_{cb} \\ V_{td} & V_{ts} & V_{tb} \end{pmatrix}$$

$$\bar{\rho} + i\bar{\eta} := 1 + \frac{V_{td}V_{tb}^*}{V_{cd}V_{cb}^*} = -\frac{V_{ud}V_{ub}^*}{V_{cd}V_{cb}^*}$$

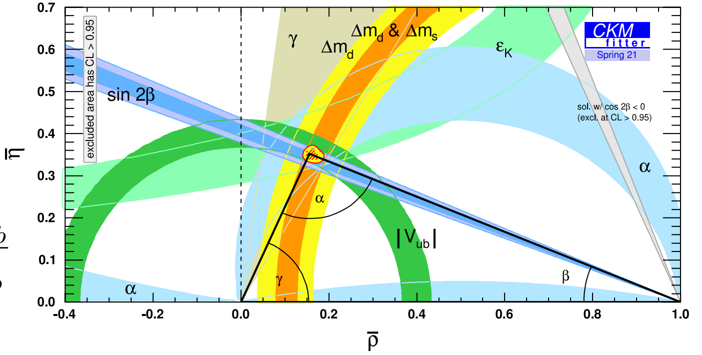

The most popular unitarity triangle illustrates unitarity constraint on the first and third columns of the CKM matrix

Wolfenstein parametrization of the CKM matrix

$$\begin{pmatrix} V_{ud} & V_{us} & V_{ub} \\ V_{cd} & V_{cs} & V_{cb} \\ V_{td} & V_{ts} & V_{tb} \end{pmatrix} = \begin{pmatrix} 1-\lambda^2/2 & \lambda & A\lambda^3(\rho - i\eta) \\ -\lambda & 1-\lambda^2/2 & A\lambda^2 \\ A\lambda^3(1-\rho-i\eta) & -A\lambda^2 & 1 \end{pmatrix} + \mathcal{O}(\lambda^4)$$

$$\lambda := \frac{|V_{us}|}{\sqrt{|V_{ud}|^2 + |V_{us}|^2}} \qquad A\lambda := \left|\frac{V_{cb}}{V_{us}}\right| \qquad A\lambda^3(\rho + i\eta) := V_{ub}^*$$

Wolfenstein parametrization highlights the size hierarchy of the CKM matrix elements

References for perturbative ingredients

- 1-loop $B \to X_s\gamma$ hard function [C.W.Bauer, S.Fleming, D.Pirjol, I.W.Stewart: hep-ph/0011336]
  [S.W.Bosch, B.O.Lange, M.Neubert, G.Paz: hep-ph/0402094]
- 2-loop $B \to X_s\gamma$ in full QCD [K.Melnikov, A.Mitov: hep-ph/0505097]
- 2-loop $B \to X_u l\bar{\nu}$ hard function [H. M. Asatrian, C. Greub, B.D.Pecjak: 0810.0987]
  [G.Bell: 0810.5695]
  [M.Beneke, T.Hubera, Xin-Qiang Li: 0810.1230]
- 1-loop $B \to X_u l\bar{\nu}$ in full QCD [F.De Fazio, M.Neubert: hep-ph/9905351]
- 1-loop jet and soft functions [C.W.Bauer, A.V.Manohar: hep-ph/0312109]
- 2-loop jet function [T.Becher, M.Neubert: hep-ph/0603140]
- 3-loop jet function [R.Brüser, Z.L.Liu, M.Stahlhofen: 1804.09722]
- 2-loop soft function [T.Becher, M.Neubert: hep-ph/0512208]
- 3-loop soft function [R.Brüser, Z.L.Liu, M.Stahlhofen: 1911.04494]
- 4-loop $\Gamma_{\rm cusp}$ [A.Manteuffel, E.Panzer, R.M.Schabinger: 2002.04617]
- 4-loop $\Gamma_{\rm cusp}$ [R.Brüser, A.Grozin, J.M.Henn, M.Stahlhofen: 1902.05076]

$$\int_0^\infty F(k)\mathrm{d}k = 1$$

$$\int_0^\infty F(k)k\mathrm{d}k = m_B - m_b$$

$$\int_0^\infty F(k)k^2\mathrm{d}k = (m_B - m_b)^2 - \frac{\lambda_1}{3}$$

$$\int_0^\infty F(k)k^3\mathrm{d}k = (m_B - m_b)^3 - \lambda_1(m_B - m_b) + \frac{\rho_1}{3}$$

Hadronic soft:

$$(S \otimes F)(k) = \langle B|\bar{b}_v \delta((n, iD) - (m_B - m_b) + k) b_v|B\rangle$$

Hadronic parameters:

$$\langle B|\bar{b}_v (iD_\alpha)(iD_\mu)(iD_\beta) b_v|B\rangle = \frac{\rho_1}{3}(g_{\alpha\beta} - v_\alpha v_\beta)v_\mu$$

$$\langle B|\bar{b}_v (iD)^2 b_v|B\rangle = \lambda_1$$

$$m_b^{\text{pole}} = \widehat{m}_b + \delta m_b$$

$$\lambda_1^{\text{pole}} = \widehat{\lambda}_1 + \delta\lambda_1$$

$$\rho_1^{\text{pole}} = \widehat{\rho}_1 + \delta\rho_1$$

parameters in "pole" scheme have a renormalon ambiguity

parameters in a short-distance scheme are renormalon-free

Corrections are series in $\alpha_s(\mu_S)$

$$F^{\text{pole}} = \left[1 + \delta m\partial + \left(\delta m^2 - \frac{\delta\lambda_1}{3}\right)\frac{\partial^2}{2} + \left(\delta m^3 - \delta m\delta\lambda_1 - \frac{\delta\rho_1}{3}\right)\frac{\partial^3}{2}\right] F$$

To avoid this problem we redefine the shape function such that its moments are given in terms of renormalon-free parameters $\widehat{m}_b, \hat{\lambda}_1, \hat{\rho}_1$.

$$F^{\text{pole}} = \left[1 + \delta m \partial + \left(\delta m^2 - \frac{\delta\lambda_1}{3}\right)\frac{\partial^2}{2} + \left(\delta m^3 - \delta m \delta\lambda_1 - \frac{\delta\rho_1}{3}\right)\frac{\partial^3}{2}\right] F$$

$$\underbrace{S^{\text{pole}} \otimes F^{\text{pole}}}_{\text{Hadronic soft function}} = S^{\text{pole}} \otimes \left[(1 + \delta m \partial + \ldots) F\right] = \underbrace{\left[(1 + \delta m \partial + \ldots) S^{\text{pole}}\right]}_{\text{renormalon ambiguity cancels}} \otimes F = S \otimes F$$

The renormalon ambiguity cancels between the correction series δm_b, $\delta\lambda_1$, $\delta\rho_1$ and the series of the partonic soft function S

Hard function

the only unknown term — fixed by RGE $\dfrac{\partial H(\mu)}{\partial \ln\mu} = \gamma_H \times H$

$$H(\mu) = 1 + \frac{\alpha_s(\mu)}{\pi} h_1 + \left(\frac{\alpha_s(\mu)}{\pi}\right)^2 h_2 + \left(\frac{\alpha_s(\mu)}{\pi}\right)^3 h_3 + \text{terms with logs } \ln\frac{\mu}{m_b} + \mathcal{O}(\alpha_s^4)$$

$$h_3 \sim \frac{{h_2}^2}{h_1} \approx \frac{19.3^2}{4.55} \approx 80 \implies h_3 = 0 \pm 80$$

For the hard function H the only missing piece is the 3-loop constant h_3.
We set its central value to 0 and use Padé approximation to estimate its possible magnitude.

singular without resummation

$x = 1 - \frac{2E_\gamma}{m_b} \in [0,1]$

$$W_{\rm s}(x) = \frac{\alpha_s}{\pi}\sigma_{\rm s}^{(1)}(x) + \left(\frac{\alpha_s}{\pi}\right)^2 \sigma_{\rm s}^{(2)}(x) + \left(\frac{\alpha_s}{\pi}\right)^3 \sigma_{\rm s}^{(3)}(x) + \text{terms with } \ln\frac{\mu}{m_b} + \mathcal{O}(\alpha_s^4)$$

$$W_{\rm ns}(x) = \frac{\alpha_s}{\pi}\sigma_{\rm ns}^{(1)}(x) + \left(\frac{\alpha_s}{\pi}\right)^2 \sigma_{\rm ns}^{(2)}(x) + \left(\frac{\alpha_s}{\pi}\right)^3 \sigma_{\rm ns}^{(3)}(x) + \text{terms with } \ln\frac{\mu}{m_b} + \mathcal{O}(\alpha_s^4)$$

nonsingular

unknown function

parameterize $\sigma_{\rm ns}^{(3)}(x) = -\sigma_{\rm s}^{(3)}(1) + \sum_{k=0}^{5} c_k L^k(x)$

model cancellation between singular and nonsingular in the tail region $(x \to 1)$

$$L(x) := \frac{1}{4}\sigma_{\rm ns}^{(1)}(x) - \frac{9}{16}$$

For the nonsingular terms $W_{\rm ns}$ only the 3-loop function $\sigma_{\rm ns}^{(3)}(x)$ is unknown.
We parameterize it using six parameters $c_0 \ldots c_5$.

Nonsingular terms

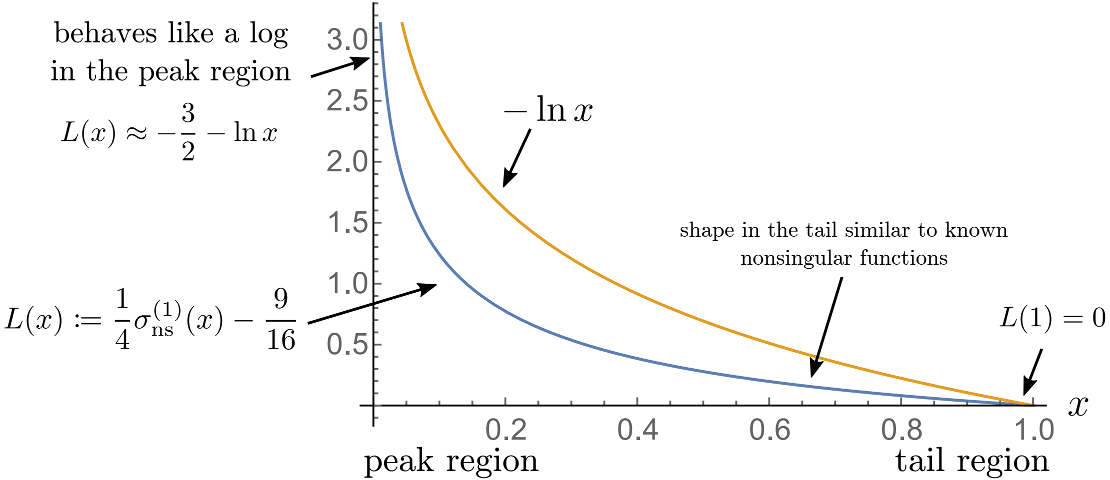

The function $L(x)$ used in the parameterization is similar to $-\ln x$, but has a more realistic shape in the transition region $0 < x < 1$.

In the peak region, where $x \to 0$:

$$
\begin{aligned}
4x\sigma_{\rm s}^{(1)}(x) &\approx -7.0 - 4\ln x \\
\sigma_{\rm ns}^{(1)}(x) &\approx -3.8 - 4\ln x
\end{aligned}
\quad \text{similar}
$$

$$
\begin{aligned}
4x\sigma_{\rm s}^{(2)}(x) &\approx 28.8 + 46.7\ln x + 26.5\ln^2 x + 2.7\ln^3 x \\
\sigma_{\rm ns}^{(2)}(x) &\approx 16.1 + 33.9\ln x + 25\ln^2 x + 2.7\ln^3 x
\end{aligned}
\quad \text{similar}
$$

$$
\begin{aligned}
4x\sigma_{\rm s}^{(3)}(x) &\approx 406.3 + 142.5\ln x - 113.2\ln^2 x - 125.5\ln^3 x - 21.7\ln^4 x - 0.9\ln^5 x \\
&\approx 258.5 + 95.0L(x) + 189.0L^2(x) + 15.5L^3(x) - 15L^4(x) + 0.9L^5(x) \\
\sigma_{\rm ns}^{(3)}(x) &= c_0 + c_1 L(x) + c_2 L^2(x) + c_3 L^3(x) + c_4 L^4(x) + c_5 L^5(x) - \sigma_{\rm s}^{(3)}(1)
\end{aligned}
$$

$c_0 = 0 \pm 20$ (estimated differently) $\quad c_1 = 0 \pm 100 \quad c_2 = 0 \pm 80 \quad c_3 = 0 \pm 10 \quad c_4 = 0 \pm 5 \quad c_5 = 0 \pm 1$

The asymptotics of nonsingular functions $\sigma_{\rm ns}^{(k)}(x)$ are similar to asymptotics of $4x\sigma_{\rm s}^{(k)}$.
We exploit this to estimate the possible magnitude of model coefficients c_k.

$$\sigma_{\mathrm{s}}^{(1)}(1) + \sigma_{\mathrm{ns}}^{(1)}(1) = \frac{9}{4} - \frac{7}{4} = \frac{1}{2}$$

$$\sigma_{\mathrm{s}}^{(2)}(1) + \sigma_{\mathrm{ns}}^{(2)}(1) \approx 7.20 - 4.28 = 2.92$$

$$c_0 = \sigma_{\mathrm{s}}^{(3)}(1) + \sigma_{\mathrm{ns}}^{(3)}(1) \approx 101.57 + ? \quad \text{expect } c_0 \approx \frac{2.92^2}{0.5} \approx 20$$

There's a somewhat large finite cancellation between singular and nonsingular in the tail region, where $x \to 1$

$$\frac{\mathrm{d}^3\Gamma}{\mathrm{d}p_X^+\,\mathrm{d}p_X^-\,\mathrm{d}E_l} \propto \underbrace{W_{\mu\nu}}_{\substack{\text{hadronic tensor}\\ \text{(difficult)}}} \overbrace{(p_X^+, p_X^-)}^{\text{no } E_l} \underbrace{L^{\mu\nu}}_{\substack{\text{leptonic tensor}\\ \text{(easy)}}} (p_X^+, p_X^-, E_l)$$

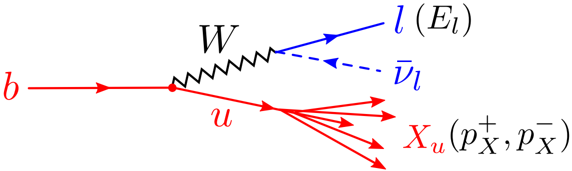

kinematically allowed phasespace

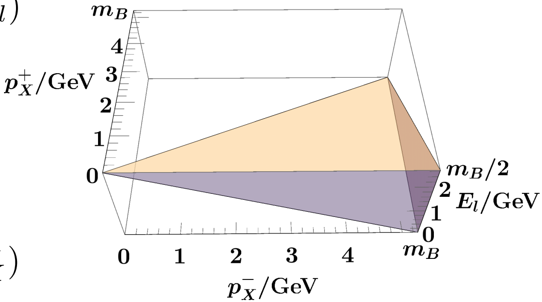

The hadronic tensor $W_{\mu\nu}$ in inclusive $B \to X_u l\bar{\nu}$ depends only on the momentum (p_X^+, p_X^-) of the final hadronic state X_u, and does not depend on the lepton energy E_l.

$$d\Gamma \propto \left(W_{\text{resum}}(\mu_H, \mu_J, \mu_S) + W_{\text{ns}}(\mu_{\text{ns}})\right) \otimes F$$

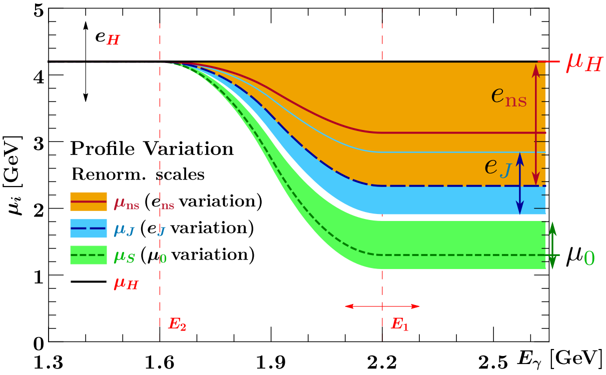

$$\mu_H = e_H m_b$$

$$\mu_{\text{ns}}(E_\gamma) = \mu_S(E_\gamma)^{\frac{1-e_{\text{ns}}}{4}} \mu_H^{\frac{3+e_{\text{ns}}}{4}}$$

$$\mu_J(E_\gamma) = \mu_S(E_\gamma)^{\frac{1-e_J}{2}} \mu_H^{\frac{1+e_J}{2}}$$

$\mu_S(E_\gamma)$ interpolates between μ_0 and μ_H

We use profile functions to smoothly turn off the resummation away from the peak region by setting all scales to the same value. The profile functions depend on parameters e_H, e_{ns}, e_J, μ_0, E_1, which are varied to estimate the perturbative uncertainty

$B \to X_u l \bar{\nu}$ profile functions

$$\mathrm{d}\Gamma \propto \left(W_{\mathrm{resum}}(\mu_H, \mu_J, \mu_S) + W_{\mathrm{ns}}(\mu_{\mathrm{ns}})\right) \otimes F$$

$$\mu_H = e_H m_b$$

$$\mu_{\mathrm{ns}}(E_\gamma) = \mu_S(E_\gamma)^{\frac{1-e_{\mathrm{ns}}}{4}} \mu_H^{\frac{3+e_{\mathrm{ns}}}{4}}$$

$$\mu_J(E_\gamma) = \mu_S(E_\gamma)^{\frac{1-e_J}{2}} \mu_H^{\frac{1+e_J}{2}}$$

$\mu_S(E_\gamma)$ interpolates between μ_0 and μ_H

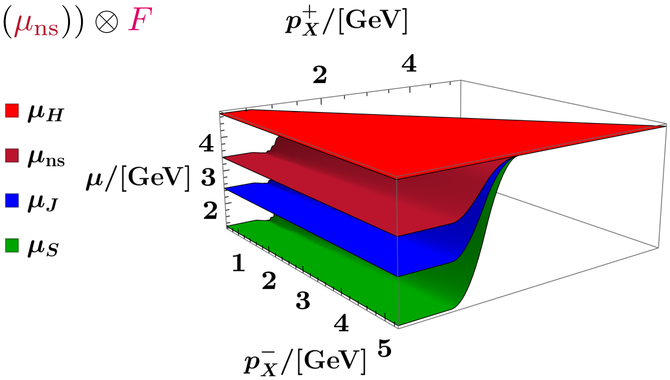

We use profile functions to smoothly turn off the resummation away from the peak region by setting all scales to the same value. The profile functions depend on parameters e_H, e_{ns}, e_J, μ_0, e^{resum}, p_X^{resum}, e^{FO}, p_X^{FO}, which are varied to estimate the perturbative uncertainty

$B \to X_u l\bar{\nu}$ boundaries of resummation and fixed-order regions

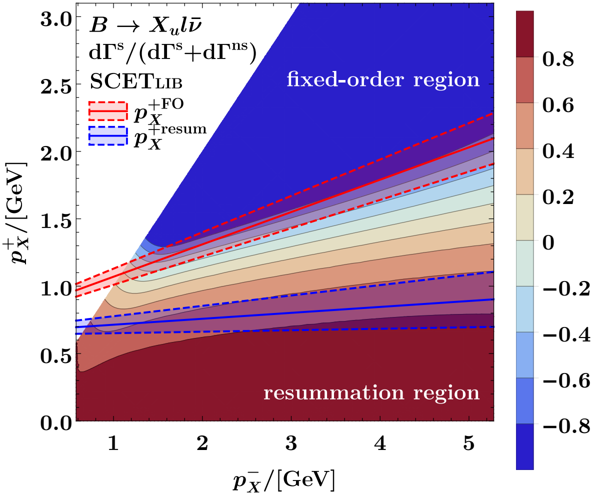

The edges of resummation and fixed-order regions are determined by examining $r = \frac{\text{singular}}{\text{singular+nonsingular}}$. The nominal edges are chosen to correspond to $r = 3/4$ and $r = -4/5$.

$$\Delta_{\text{total}} = \sqrt{\Delta^2_{\text{resum}} + \Delta^2_{\text{ns}} + \Delta^2_{\text{match}} + \underbrace{\Delta^2_{h_3} + \textstyle\sum_{k=0}^{5} \Delta^2_{c_k}}_{\substack{\text{variations of nuisance parameters} \\ \text{(only for } B \to X_s\gamma \text{ at N}^3\text{LO)}}}}$$

$$\begin{aligned}
\Delta_{\text{resum}} &= \text{envelope of } (e_H, e_J, \mu_0) \text{ variations} \\
&= \text{scale variations in resummed and fixed-order terms} \\
\Delta_{\text{ns}} &= \Delta_{e_{\text{ns}}} = \text{scale variations in nonsingular terms} \\
\Delta_{\text{match}} &= \text{variations of transition points between resummed and fixed-order regions}
\end{aligned}$$

Uncertainty is estimated as a sum in quadrature of resummation, nonsingular, matching, and nuisance-parameter uncertainty.

$B \to X_s\gamma$ components of relative uncertainty

$$\Delta_{\rm total} = \sqrt{\Delta^2_{\rm resum} + \Delta^2_{\rm ns} + \Delta^2_{\rm match} + \Delta^2_{h_3} + \Delta^2_{c^{\rm ns}}}$$

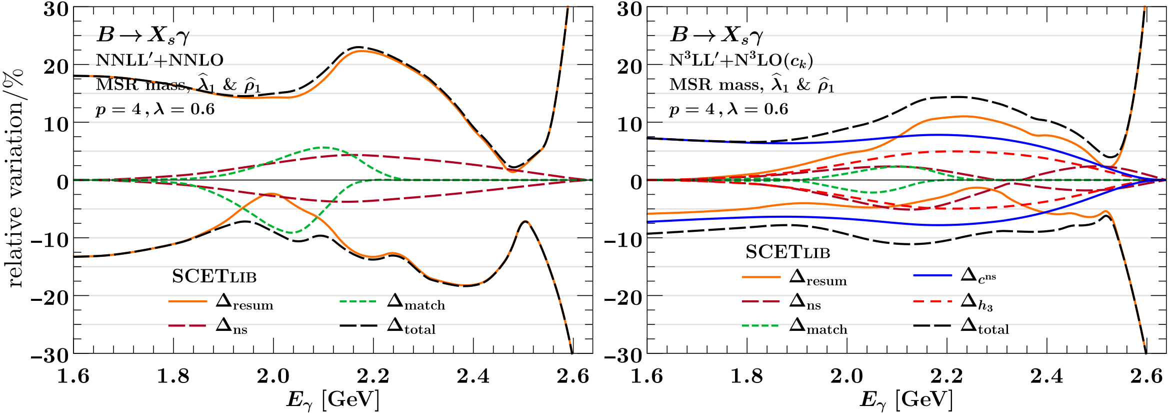

The unknown 3-loop nonsingular terms are not relevant in the peak region,
but increase the uncertainty towards the tail

$B \to X_u l \bar{\nu}$ lepton energy spectrum: MSR vs $1\mathrm{S}$ scheme

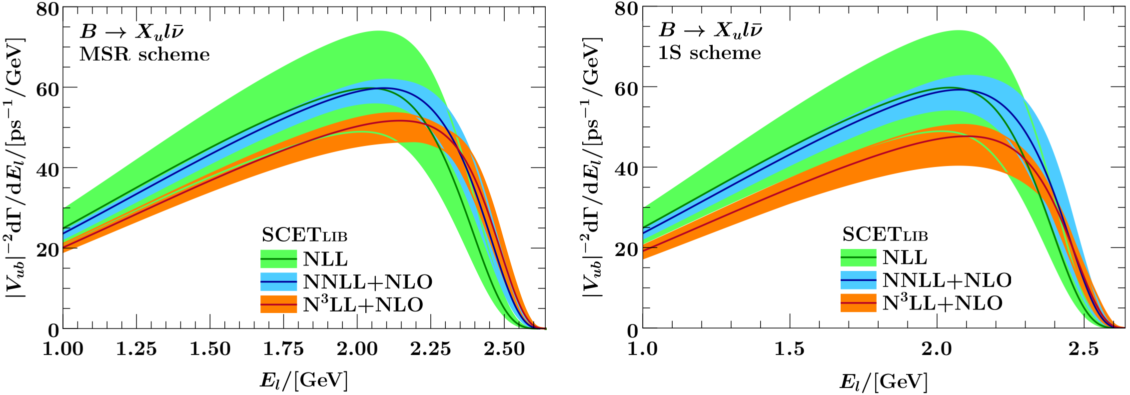

The results in the MSR and $1\mathrm{S}$ schemes are similar.

$B \to X_u l \bar{\nu}$ lepton energy spectrum: MSR vs 1S scheme

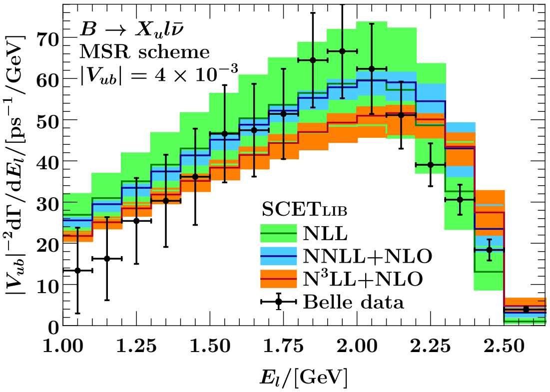

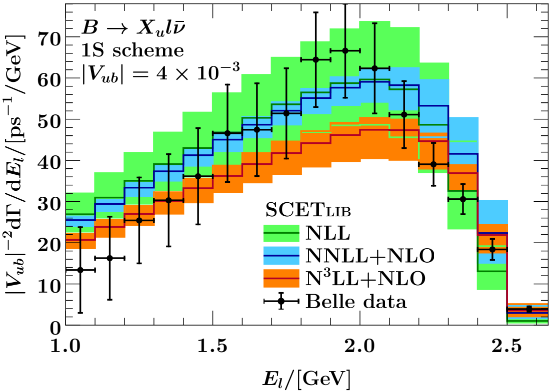

The results in the MSR and 1S schemes are similar.

$B \to X_u l\bar{\nu}$ p_X^+ spectrum: MSR vs $\mathrm{1S}$ scheme

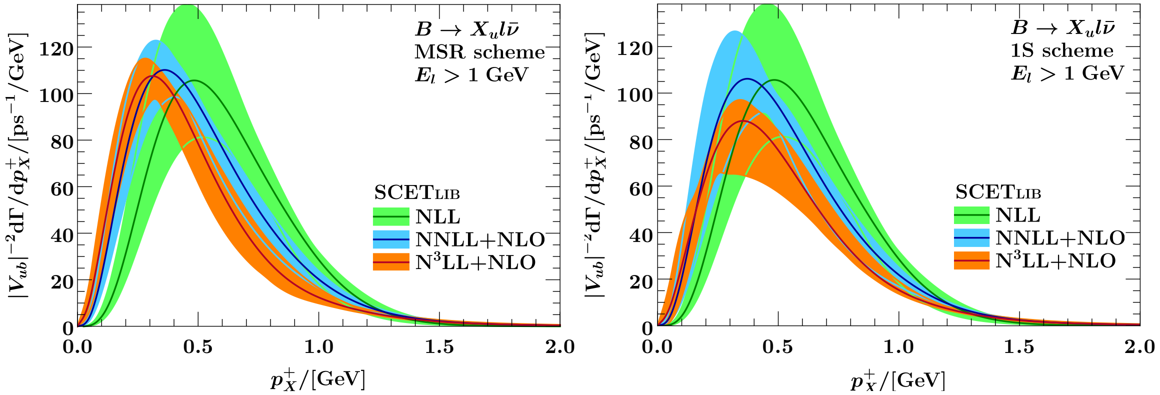

The convergence in the MSR scheme is a bit better than in the $\mathrm{1S}$ scheme.

$B \to X_u l\bar{\nu}$ p_X^+ spectrum: MSR vs 1S scheme

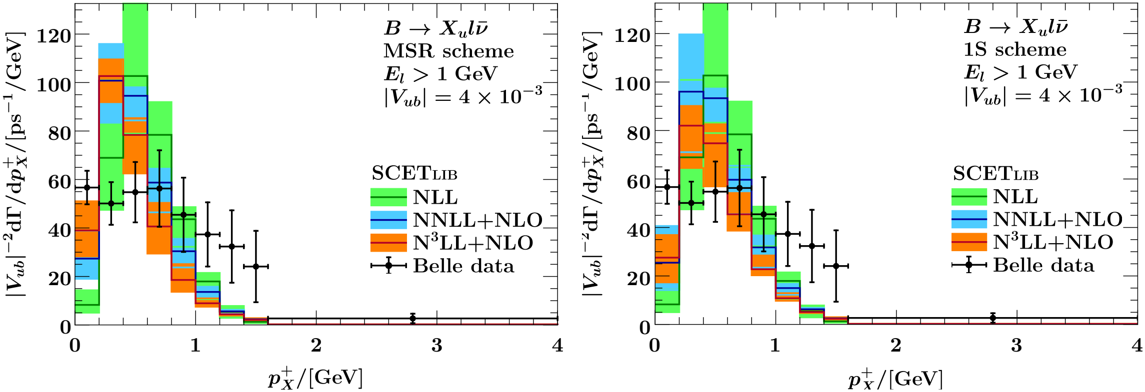

The difference between MSR and the 1S does not explain the disagreement with the data at $p_X^+ > 1\,\mathrm{GeV}$.

Convergence problem in the 1S scheme

$$m_b^{\rm pole} - m_b^{1S} =: \delta m_b^{1S}(\mu) = R^{1S}(\mu)\left(\sum_{k=1}^{3}\left(\frac{\alpha_s(\mu)}{\pi}\right)^k a_{1S}^{(k)} + \text{terms with } \ln\frac{\mu}{R^{1S}(\mu)} + \mathcal{O}(\alpha_s^4)\right)$$

intrinsic scale of 1S mass scheme

[K.Melnikov, A.Yelkhovsky: hep-ph/9805270]

[A.Pineda, F.J.Ynduráin: hep-ph/9711287]

$$R^{1S}(\mu) = m_b^{1S}\alpha_s(\mu)C_F$$

$$R^{1S}(m_b^{1S}) \approx R^{1S}(4.75) \approx 1.36 \sim \mu_S \qquad \text{ok!}$$

$$R^{1S}(\mu_S) \approx R^{1S}(1.3) \approx 2.4 \gg \mu_S \qquad \text{too large!}$$

(all values in GeV)

This is because the intrinsic scale of 1S scheme R^{1S}
is small at the hard scale, but becomes too large at the soft scale

$$R^{\mathrm{MSR}} = \mu \qquad\qquad \sim \alpha_s \quad \sim \alpha_s^2 \quad \sim \alpha_s^3$$

$$(m_b^{\mathrm{MSR}} - m_b^{1S})(\mu = \mu_H) \approx -0.35 - 0.12 - 0.04 \leftarrow \text{converges}$$

$$(m_b^{\mathrm{MSR}} - m_b^{1S})(\mu = \mu_J) \approx -0.15 - 0.06 + 0.02 \leftarrow \text{converges}$$

$$(m_b^{\mathrm{MSR}} - m_b^{1S})(\mu = \mu_S) \approx -0.06 - 0.06 + 0.10 \leftarrow \text{does not converge}$$

(all values in GeV)

The perturbative series of correction between MSR and 1S schemes seems to start diverging as the scale μ approaches the soft scale μ_S.

$B \to X_u l\bar{\nu}$ lepton energy spectrum with SIMBA shape function

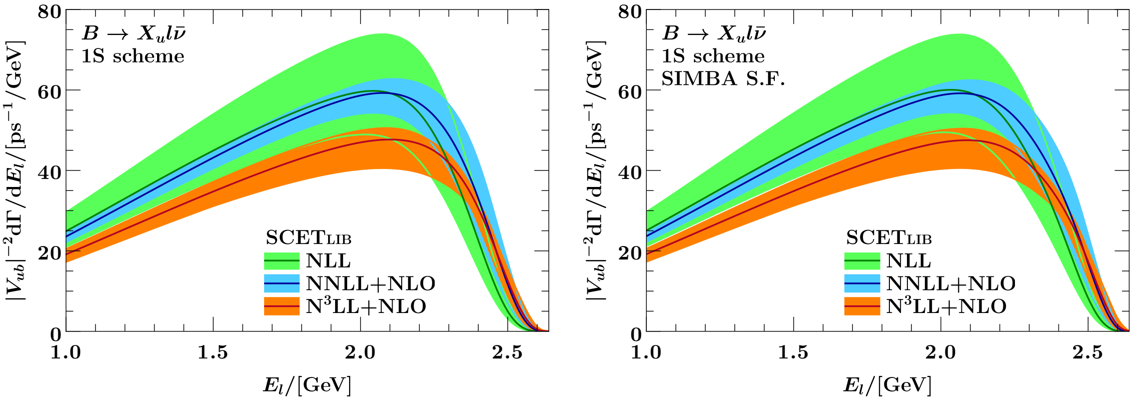

The default shape function is already close to the shape function fitted by SIMBA.
The results with the SIMBA shape function are similar.

$B \to X_u l\bar{\nu}$ lepton energy spectrum with SIMBA shape function

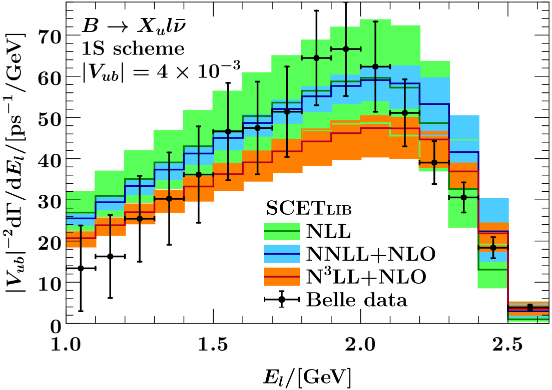

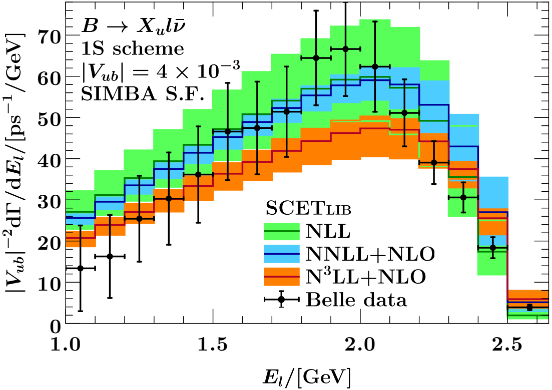

The default shape function is already close to the shape function fitted by SIMBA.
The results with the SIMBA shape function are similar.

$B \to X_u l\bar{\nu}$ lepton energy spectrum with SIMBA shape function

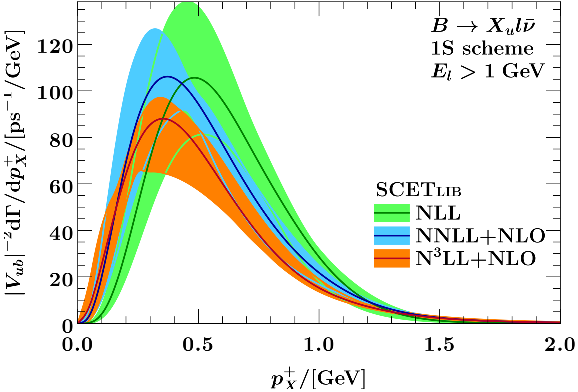

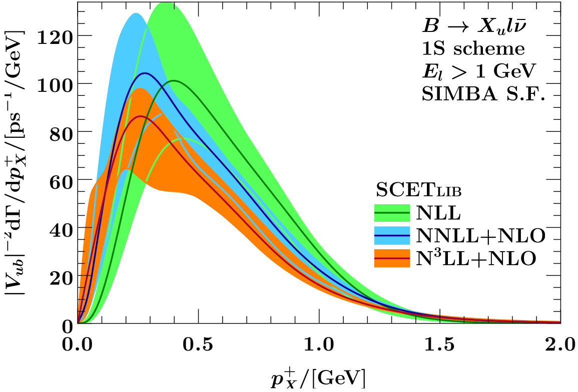

The default shape function is already close to the shape function fitted by SIMBA.
The results with exactly the SIMBA shape function are similar.

$B \to X_u l\bar{\nu}$ lepton energy spectrum with SIMBA shape function

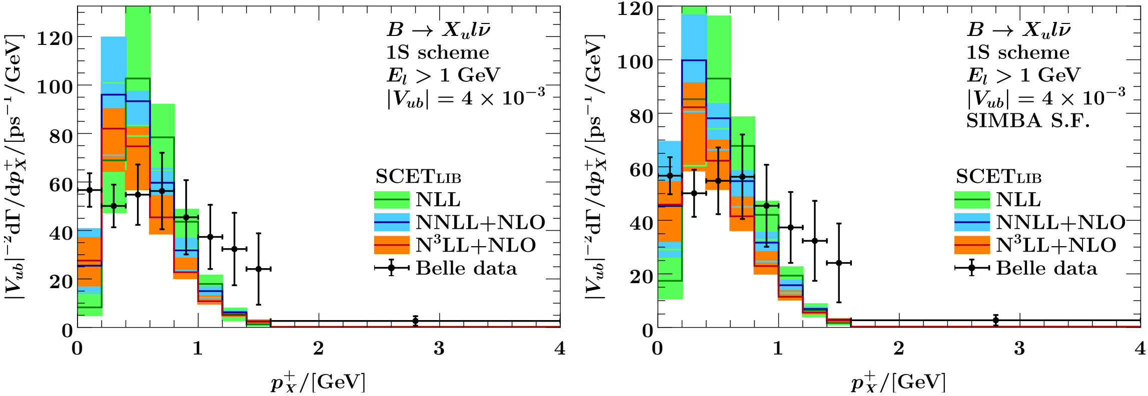

The default shape function is already close to the shape function fitted by SIMBA.
The results with exactly the SIMBA shape function are similar.

$B \to X_u l\bar{\nu}$ p_X^- spectrum

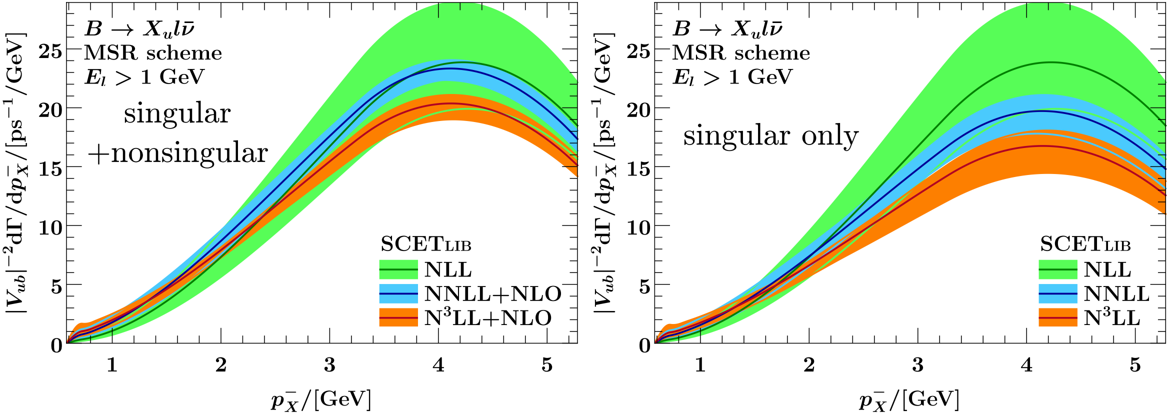

It is important to include nonsingular corrections. Because of the missing NNLO nonsingular corrections the N^{3}LL+NLO results do not agree with lower orders.

$B \to X_u l\bar{\nu}$ q^2 spectrum

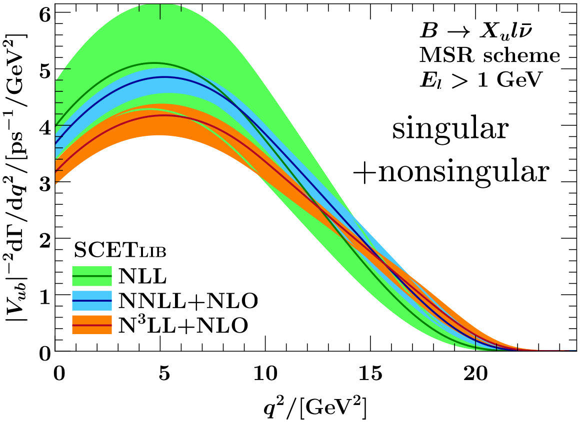

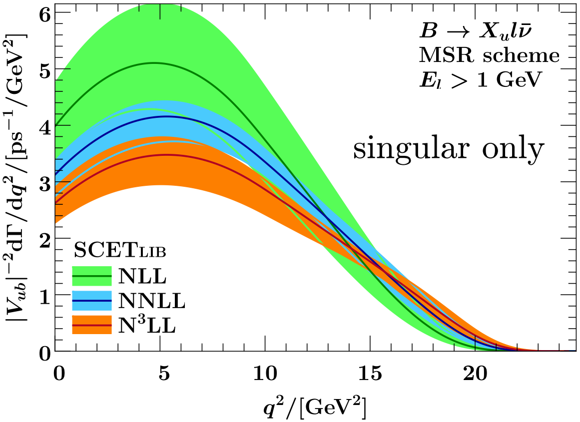

Nonsingular corrections are important. The $\mathrm{N^3LL+NLO}$ results do not agree with lower orders because of the missing 2-loop nonsingular corrections.

Belle data from [Phys.Rev.Lett. 127 (2021) 26, 261801, Belle coll

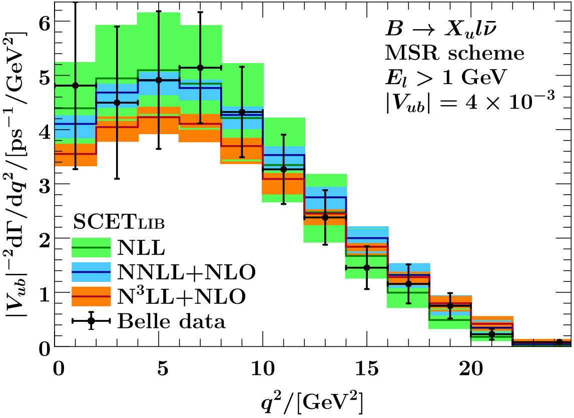

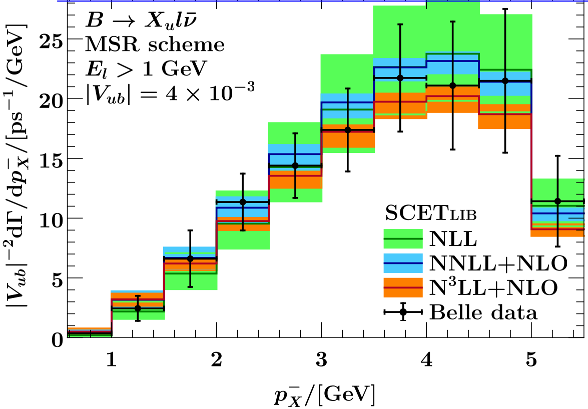

The $\mathrm{d}\Gamma/\mathrm{d}q^2$ and $\mathrm{d}\Gamma/\mathrm{d}p_X^-$ spectra, which are insensitive to the shape function F, agree with Belle measurements, even at $\mathrm{N^3LL+NLO}$.

$B \to X_u l\bar{\nu}$ m_X^2 spectrum

Belle data and right plot from

[Phys.Rev.Lett. 127 (2021) 26, 261801, Belle collaborat

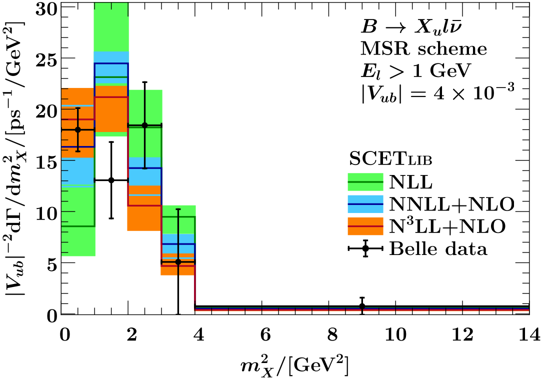

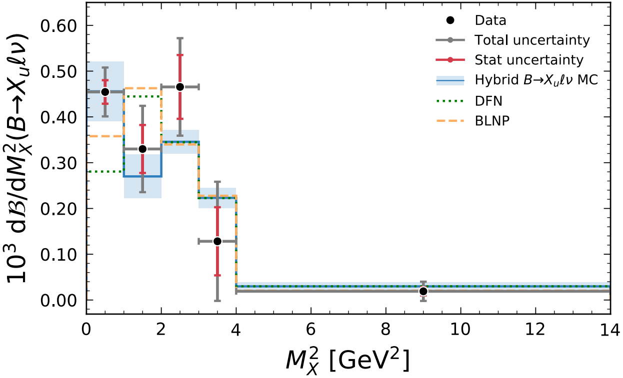

The invariant-mass-squared spectrum $\mathrm{d}\Gamma/\mathrm{d}m_X^2$ is dominated by resonances and cannot be adequately described by an inclusive model.

Tension between inclusive and exclusive determinations of $|V_{ub}|$

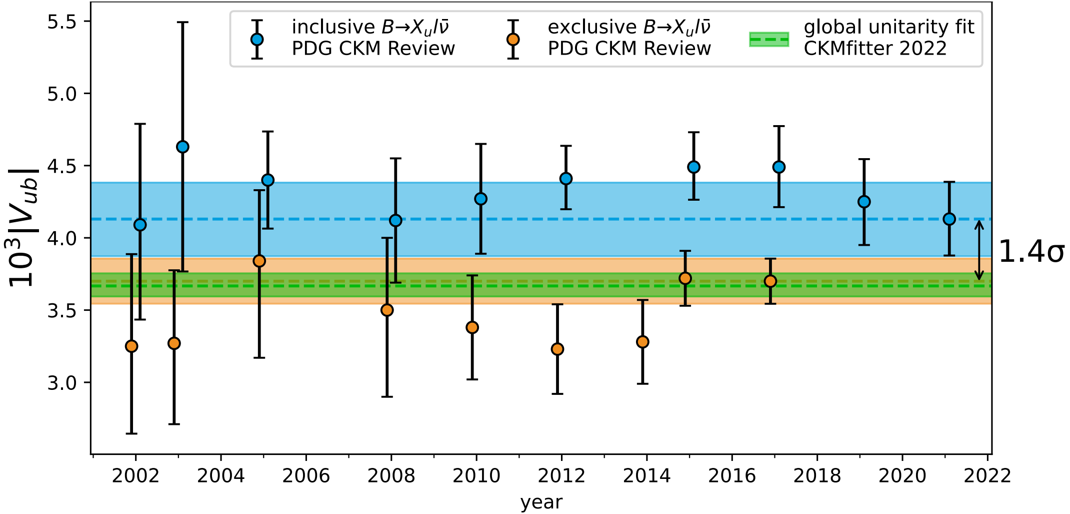

In spite of increasing precision there's a persistent tension between inclusive and exclusive determinations of $|V_{ub}|$

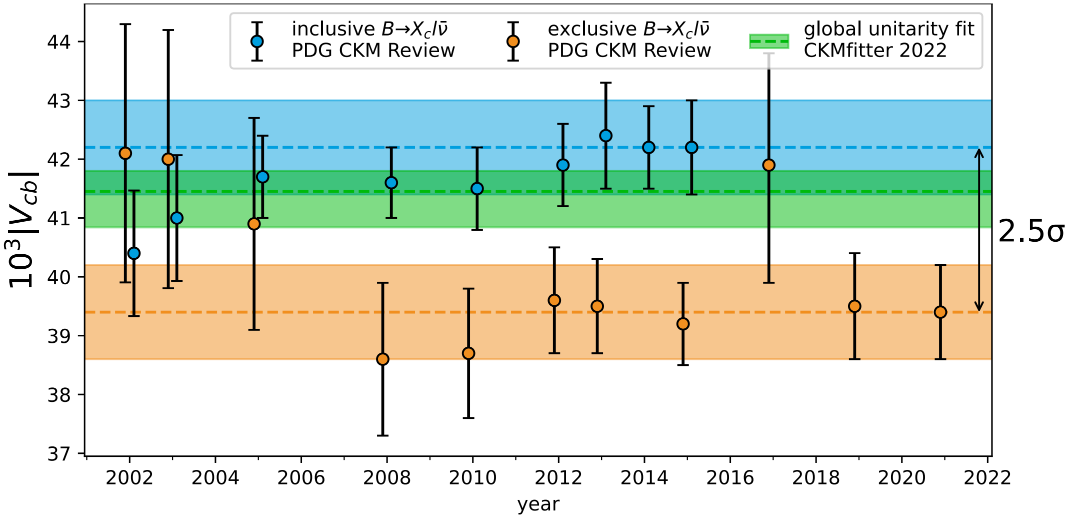

In spite of increasing precision there's a persistent tension between inclusive and exclusive determinations of $|V_{cb}|$

$$p = (E, p_x, p_y, p_z) = \frac{p^-}{2} n + \frac{p^+}{2} \bar{n} + p_\perp$$
$$n = \begin{pmatrix} 1 & 0 & 0 & 1 \end{pmatrix}$$
$$\bar{n} = \begin{pmatrix} 1 & 0 & 0 & -1 \end{pmatrix}$$

$$p^+ := (n \cdot p) = E - p_z \longleftarrow \text{small for strongly boosted}$$
$$p^- := (\bar{n} \cdot p) = E + p_z \longleftarrow \text{large for strongly boosted}$$

Lightcone coordinates p^-, p^+ are convenient, because for strongly boosted state X $p_X^- \gg p_X^+$.
Soft-Collinear Effective theory is appropriate in the region where $p_X^+/p_X^- \ll 1$.

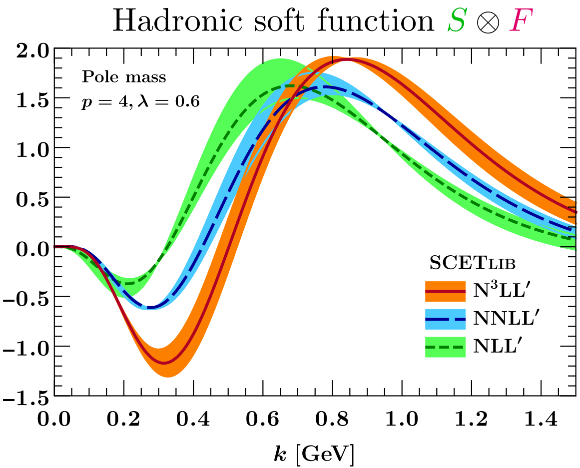

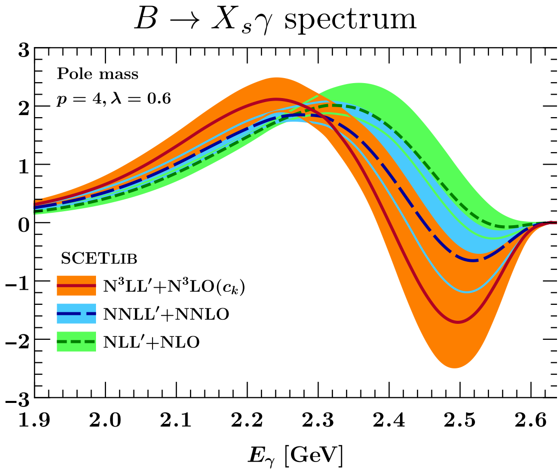

Pole mass scheme suffers from a renormalon ambiguity,
and predictions in this scheme are not stable.

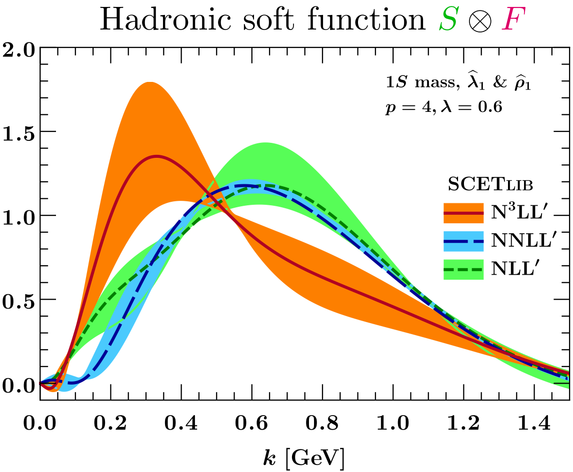

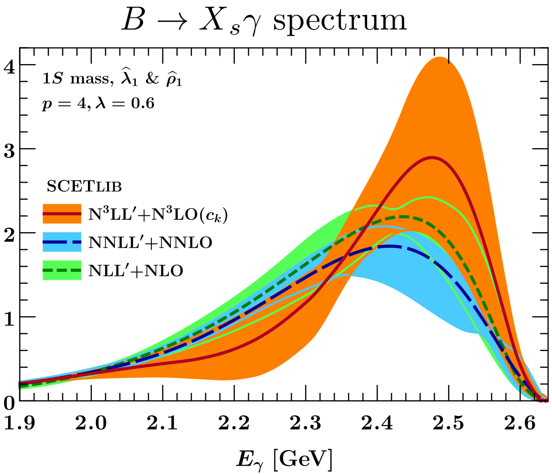

However, the 1S mass scheme, which has been used in the NNLL$'$+NNLO shape function fit in [Bernlochner et al.: 2007.04320], starts to break down at N^{3}LO

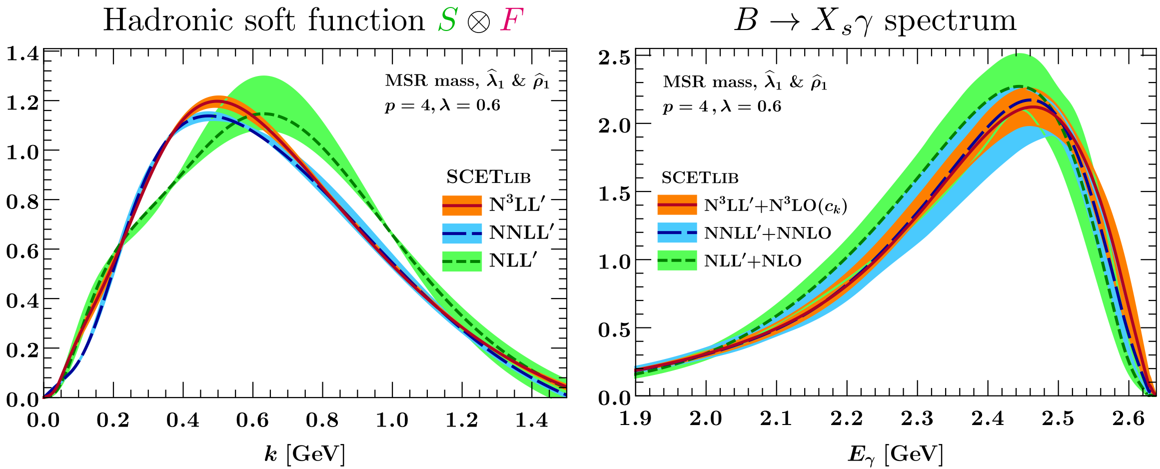

The MSR scheme yields much more stable results because we can pick the R-scale $R \sim \mu_S$

Double-differential $B \to X_u l \bar{\nu}$ decay rate

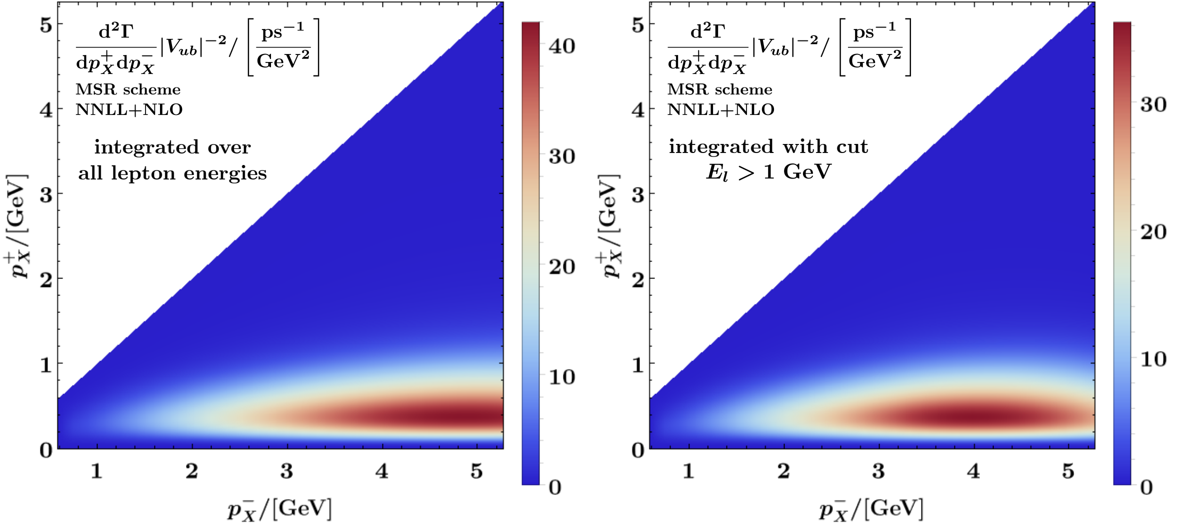

The cut $E_l > 1\,\mathrm{GeV}$ shifts the peak of the distribution towards smaller p_X^-.

Reduction of uncertainty in $B \to X_u l\bar{\nu}$ due to 2-loop singular corrections

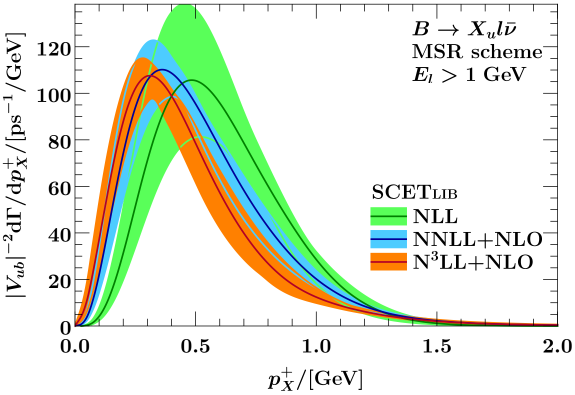

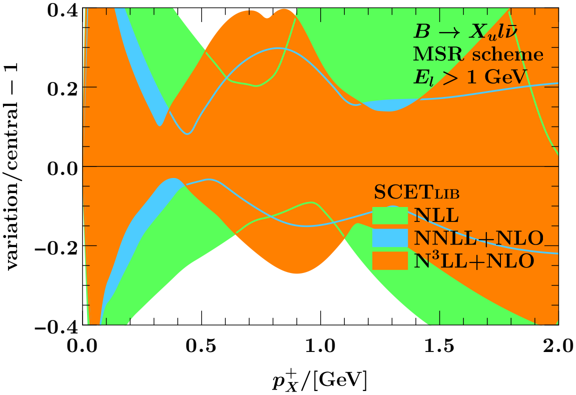

2-loop singular corrections reduce the uncertainty in the peak region from $\sim 20\%$ to $\sim 10\%$.

Impact of short-distance schemes for λ_1 and ρ_1

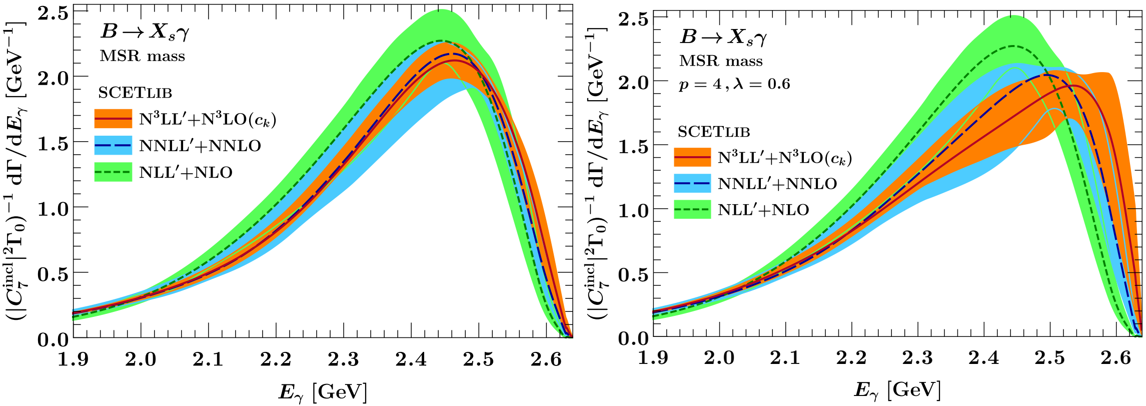

Short-distance schemes for hadronic parameters λ_1 and ρ_1 further improve the stability of the spectrum

Impact of short-distance schemes for λ_1 and ρ_1

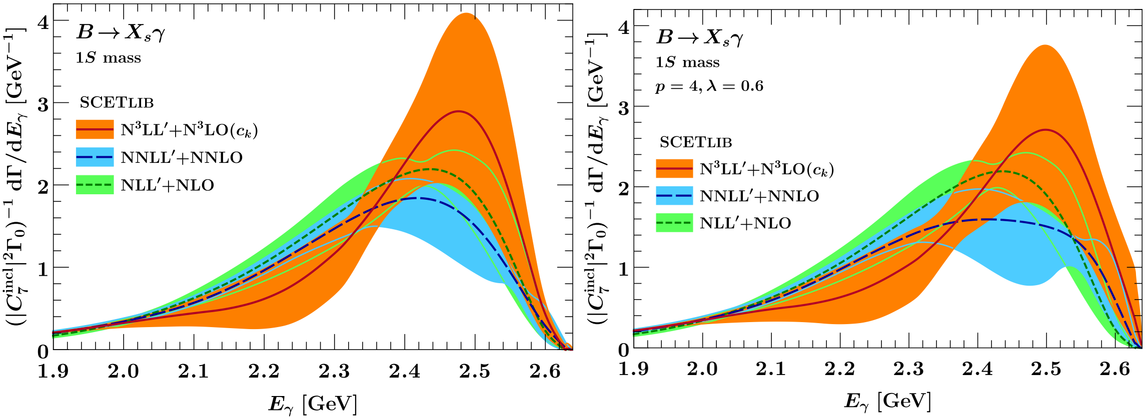

It does not seem possible to compensate the unexpectedly large correction in the 1S scheme at the 3-loop order by a judicious redefinition of λ_1 and ρ_1.